Uniqueness of the thermodynamic limit for driven disordered elastic interfaces



J. Stat. Mech. (2013) P12004

(http://iopscience.iop.org/1742-5468/2013/12/P12004)

Journal of Statistical Mechanics: Theory and Experiment
An IOP and SISSA journal

# Uniqueness of the thermodynamic limit for driven disordered elastic interfaces

**A B Kolton[1], S Bustingorry[1], E E Ferrero[1,3] and A Rosso[2]**

[1] CONICET, Centro Atómico Bariloche, 8400 San Carlos de Bariloche, Río Negro, Argentina
[2] LPTMS, Université Paris-Sud, CNRS (UMR 8626), F-91405 Orsay Cedex, France
E-mail: koltona@cab.cnea.gov.ar, sbusting@cab.cnea.gov.ar, ferrero@cab.cnea.gov.ar and alberto.rosso@u-psud.fr

Received 20 August 2013
Accepted 4 November 2013
Published 6 December 2013

Online at stacks.iop.org/JSTAT/2013/P12004
doi:10.1088/1742-5468/2013/12/P12004

**Abstract.** We study the finite-size fluctuations at the depinning transition for a one-dimensional elastic interface of size $L$ displacing in a disordered medium of transverse size $M = kL^{\zeta}$ with periodic boundary conditions, where $\zeta$ is the depinning roughness exponent and $k$ is a finite aspect-ratio parameter. We focus on the crossover from the infinitely narrow ($k \to 0$) to the infinitely wide ($k \to \infty$) medium. We find that at the thermodynamic limit both the value of the critical force and the precise behaviour of the velocity–force characteristics are *unique* and $k$-independent. We also show that the finite-size fluctuations of the critical force (bias and variance) as well as the global width of the interface cross over from a power-law to a logarithm as a function of $k$. Our results are relevant for understanding anisotropic size effects in force-driven and velocity-driven interfaces.

**Keywords:** finite-size scaling, interfaces in random media (theory), fluctuations (theory), transport properties (theory)

[3] Present address: LIPhy, Université Joseph Fourier, UMR 5588, F-38041 Grenoble CEDEX, France.


1742-5468/13/P12004+19$33.00

## Contents



## 1. Introduction

Understanding anisotropic finite-size effects in driven condensed matter systems is important not only for their custom numerical simulation analysis and modelling, but also to interpret an increasing amount of experiments performed on relatively small samples with specially devised geometries, where one of the system dimensions can be even comparable to a typical static or dynamical correlation length. The steady-state dynamics of directed elastic interfaces in random media, experimentally realized in driven ferromagnetic [1]–[5] and ferroelectric [6]–[10] domain walls, contact lines in wetting [11, 12] and fractures [13, 14], is a non-trivial relevant example where this kind of phenomenology arises. The study of driven domain wall motion in ferromagnetic micro-tracks for instance [15], relevant for memory-device applications or metallic ferromagnet spintronics [16], motivates the study of their motion in 'wide' samples, i.e. much wider than the interface global width. Moreover, at the integration scale for modern nano-devices, these tracks can also become thin enough to be comparable to the typical size of the thermal nuclei controlling creep motion, thus yielding an experimentally observable dynamical dimensional crossover [17]. At the other extreme, periodic systems such as planar vortex lattices, charge density waves, or experimental realizations of elastic chains in random media, motivate, through an appropriate mapping, the study of the motion of large interfaces in periodically repeated 'narrow' media, i.e. much narrower than the interface width [18]–[20].



J. Stat. Mech. (2013) P12004

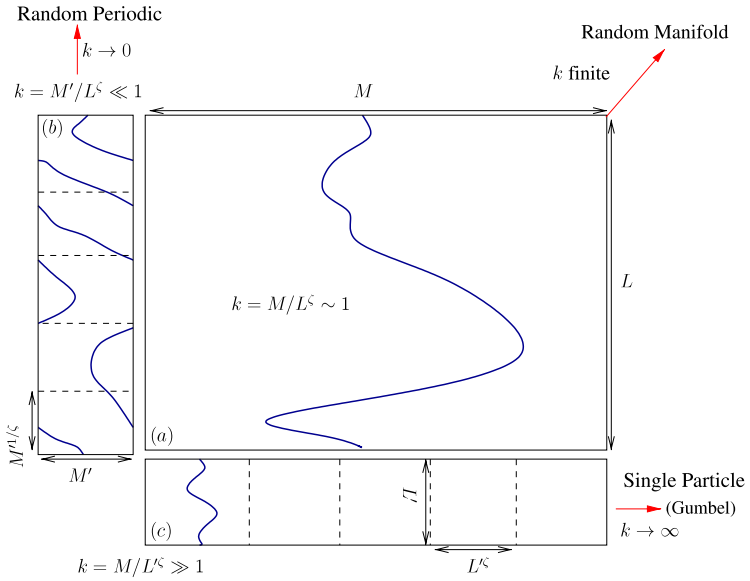


**Figure 1.** Schematic picture showing critical configurations for systems with different values of the aspect ratio $k$. In (a) the critical configuration has a width $w$ comparable to the system transverse dimension $M$. In (b), $w \gg M'$ and the configuration wraps several times, crossing over to the RP geometry, $w \sim L^{\zeta_{\rm RP}}$. In (c) $w \ll M$ and $w/L^\zeta$ is a function of $k$. In the thermodynamic limit, if $k$ is kept constant, transport properties converge to a unique RM limit. If $k \to 0$ the thermodynamic limit corresponds to the RP class parametrized by the periodicity $M'$. If $k \to \infty$ the system has a dimensional crossover towards the zero-dimensional Gumbel class (for Gaussian microscopic disorder), and the steady-state motion is static.

Minimal models, such as the paradigmatic quenched-Edwards–Wilkinson equation (QEW) and their close quenched disorder variants [21], were shown to successfully capture experimentally observed universal dynamics such as creep [1] and depinning [12, 22] phenomena. In spite of this, fundamental questions such as the possible thermodynamic limits of these models, when supplemented with the usual periodic boundary conditions, are not completely understood. Roughly speaking, the steady-state motion of extended elastic interfaces is expected to be very different in very narrow samples from in very wide samples because they actually sense rather different pinning force fluctuations from the *same* microscopic model. The thermodynamic limit in between these two extremes (i.e., neither infinitely narrow nor wide samples), hence, looks rather ambiguous [23]: it is unclear whether it leads to a unique solution or to a family of solutions parametrized by some properly defined aspect-ratio parameter.

Let us consider a driven QEW one-dimensional interface in a disordered sample of dimensions $L \times M$, with periodic boundary conditions, as schematically shown in figure 1(a). For each sample, at zero temperature, a critical force $f_{\rm c}^{\rm s}$ separates a pinned phase from a sliding phase characterized by a finite velocity $v^{\rm s}$. In finite systems, both $f_{\rm c}^{\rm s}$ and $v^{\rm s}$ fluctuate from sample to sample and their averages over all disorder realizations, namely $\langle f_{\rm c}^{\rm s} \rangle$ and $\langle v^{\rm s} \rangle$, depend both on microscopic details of the model (microscopic disorder distribution, lattice discretization, etc) and the specific geometry of the sample



J. Stat. Mech. (2013) P12004

(boundary conditions, transverse size, etc). In [19] it was shown that if we choose $M = kL^{\zeta}$, with $\zeta$ the depinning roughness exponent, and a Gaussian microscopic disorder, the critical force distribution crosses over from a Gaussian (for $k \to 0$) to a Gumbel distribution (for $k \to \infty$) in the large $L$ limit. One can show that the 'infinitely narrow' $k \to 0$ limit corresponds to the so-called random periodic (RP) depinning universality class, while the 'infinitely wide' $k \to \infty$ limit corresponds to a dimensional crossover towards the zero-dimensional case describing a single particle in an effective one-dimensional potential. In the former case, periodic effects arise when $M$ turns out to be comparable to the interface width, and becomes more and more important as $k$ decreases further and the interface winds more around the cylinder with perimeter $M$, as schematically shown in figure 1(b). In the latter case instead, as schematically shown in figure 1(c), periodicity effects are absolutely negligible but the roughness turns anomalous due to extreme value statistics effects [24]. In fact, for fixed $L$ and Gaussian disorder, $\langle f_{\mathrm{c}}^{\mathrm{s}} \rangle \to \infty$ as $M \to \infty$; so that, at zero temperature, a finite velocity is only possible in a non-steady-state [25]. The so-called random manifold (RM) regime, which exists between these two extreme limits for any finite $k$, was shown to display a *finite* critical force $f_{\mathrm{c}}$ in the thermodynamic limit ($f_{\mathrm{c}} = \lim_{L\to\infty} \langle f_{\mathrm{c}}^{\mathrm{s}} \rangle$), with sample to sample fluctuations vanishing as [19, 26, 27] $\langle [f_{\mathrm{c}}^{\mathrm{s}} - \langle f_{\mathrm{c}}^{\mathrm{s}} \rangle]^2 \rangle \sim L^{-2/\nu} = L^{-2(2-\zeta)}$, given the STS relation $\nu = 1/(2-\zeta)$. Finite-size effects in a discrete version of the QEW model were also tackled in a very recent paper, [28], but in a different framework. In that approach, the critical force is defined as the threshold needed to attain a given 'target' for the mean interface position, and boundary conditions are open in the direction of motion.

The previous results represent a considerable progress in the understanding of the finite-size effects but still leave us with a rather ambiguous picture for applications and analytical calculations. Important open questions are: (i) what is the dependence of $f_{\mathrm{c}}$, and $\langle [f_{\mathrm{c}}^{\mathrm{s}} - \langle f_{\mathrm{c}}^{\mathrm{s}} \rangle]^2 \rangle$, with the self-affine aspect-ratio parameter $k$? (ii) is there a finite-size bias $[f_{\mathrm{c}} - \langle f_{\mathrm{c}}^{\mathrm{s}} \rangle]$ and how does it depend on $L$ and $k$?. (iii) Is the RM thermodynamic limit prescription for the critical force, $\lim_{L,M=kL^{\zeta}\to\infty}$, different from the one for extracting the RM velocity–force characteristics? In the affirmative case, how does it depend on $k$? (iv) Geometry and transport are closely related, as changes in the interface velocity directly affect the location of one or several geometrical crossovers [29]–[31]. How sensitive to the value of $k$ are the geometry and the velocity of the interface? In this paper we address these open questions and show that constant force simulations in finite samples actually lead to an unambiguous thermodynamic critical force and velocity–force characteristics, which are independent of $k$, as long as $k$ is finite. We also show how the finite system transport properties scale towards the (RP) $k \to 0$ and (single particle or extreme RM) $k \to \infty$ limits as a function of $L$. Finally we discuss how our results relate to the cases of velocity-driven interfaces and other alternative methods used to define the thermodynamic critical force.

## 2. Model, observables and method

We consider the driven QEW model at zero temperature, described by

$$\gamma \partial_t u(x,t) = c\partial_x^2 u(x,t) + F_p(u,x) + f. \tag{1}$$



J. Stat. Mech. (2013) P12004

This equation models the overdamped dynamics of the displacement field $u(x,t)$ of a one-dimensional elastic interface in a two-dimensional random medium. We will consider here a sample of size $L \times M$ with periodic boundary conditions in both directions. The pinning force derives from a bounded random potential (i.e. random bond disorder), $F_p(u,x) = -\partial_u U(u,x)$, with correlations

$$\langle [U(u,x) - U(u',x')]^2 \rangle = R(u-u')\delta(x-x'), \tag{2}$$

with $R(y)$ a short-ranged function of range $r_f$ and $\langle \cdots \rangle$ standing for the average over all disorder realizations.

In particular we study a model of equation (1) where the displacement field is discrete in the $x$-direction, and the random potential $U(u,x)$ is given by a sequence of uncorrelated random (Gaussian) numbers glued by a piece-wise cubic-spline with $r_f = 1$. The details of the model are described elsewhere [32]. For each sample there is a *unique* critical force $f_c^s$ and a *unique* critical configuration $u_c^s(x)$. Both quantities are computed in an efficient and accurate way without actually solving the true dynamics [32, 33]. For $f > f_c^s$, at long times, the interface acquires a steady-state velocity $v^s$. To obtain it, we solve the dynamics of equation (1) from an arbitrary initial condition up to very long times using a parallel algorithm [34]. We define the width $w$ of the critical configuration:

$$w^2(L,M) = \left\langle \frac{1}{L} \sum_{x=0}^{L-1} [u_c^s(x) - u_{cm_c}{}^s]^2 \right\rangle, \tag{3}$$

with $u_{cm_c}{}^s = (1/L)\sum_{x=0}^{L-1} u_c^s(x)$ the sample dependent centre of mass position of the critical configuration. When $M \sim L^\zeta$ it is well known that $w^2 \sim L^{2\zeta}$ with [34] $\zeta = 1.250 \pm 0.005$.

In the following, we analyse the large-size limit of (i) the critical force, (ii) the velocity for a fixed value of the external force and (iii) the width of the critical configuration, as functions of both $L$ and $k$, from the infinitely narrow sample to the infinitely wide sample.

## 3. Results

### 3.1. Summary of finite-size scaling results

Here we summarize our main results. Note that in one dimension, the roughness exponent for the RM class is [34] $\zeta = 1.250$, and for the RP class is [20, 35] $\zeta^{\mathrm{RP}} = 1.5$. A detailed description and discussion of each result is left for the next sections. The main results are:

(1) The critical force reaches a *k-independent* value $f_c = \lim_{L,M\to\infty} \langle f_c^s \rangle$ in the thermodynamic limit $L, M \to \infty$ for any *finite* $k = M/L^\zeta$ (see figure 2). This value depends only on the microscopic details of the system. The velocity–force characteristics also displays the same convergence towards a unique $k$-independent thermodynamic value, $v(f) = \lim_{L,M\to\infty} \langle v^s(f) \rangle$ (see figure 10).

(2) The average finite-size critical force $\langle f_c^s \rangle$ approaches the value $f_c$ from above if $k$ is large, and from below if $k$ is small, compared to a (non-universal) marginal value $k^* \approx 2.1 \pm 0.1$ (see figures 2 and 3). The asymptotic forms for this bias are well described by

$$(f_c - \langle f_c^s \rangle) L^{2-\zeta} \sim \begin{cases} k^{1-2/\zeta} & \text{if } k \ll k^* \\ -(\log k)^{1/\delta} & \text{if } k \gg k^* \end{cases} \tag{4}$$



J. Stat. Mech. (2013) P12004

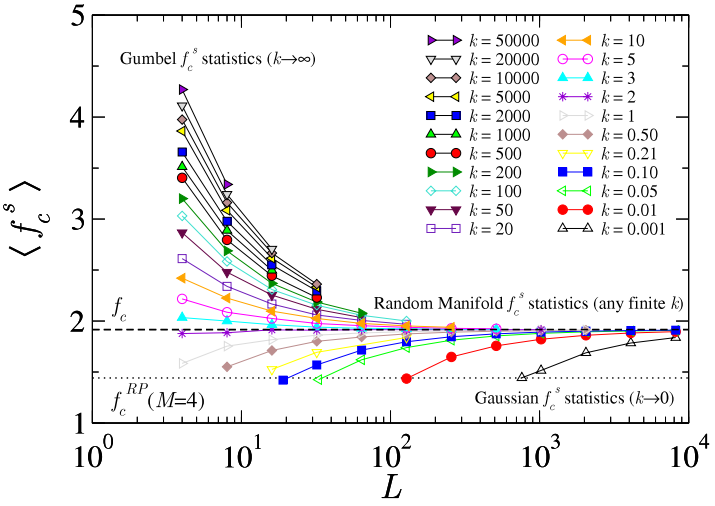


**Figure 2.** Longitudinal finite-size dependence of the averaged critical force for samples of size $L \times M$, with $M = kL^{\zeta}$. The (non-universal) thermodynamic limit $f_c$ attracts any finite value of $k$, thus determining this property unambiguously for the RM class. Also indicated is the (non-universal) thermodynamic RP critical force for a periodicity $M = 4$. Note that for $k = k^* \approx 2$, finite-size effects are negligible for several decades of $L$.

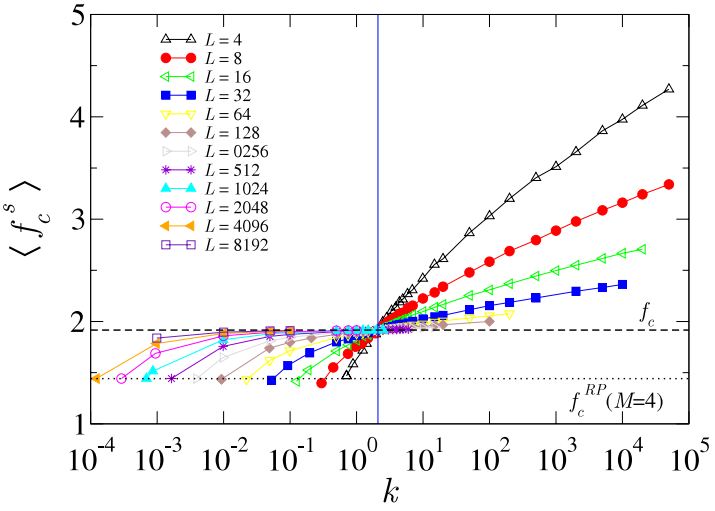


**Figure 3.** Same data as in figure 2 but showing the transverse finite-size dependence, for each $L$, of the averaged critical force. Note the crossing at $k^* \approx 2$ (precisely we get $k^* = 2.1 \pm 0.1$), bridging the Gaussian ($k \to 0$) with the Gumbel ($k \to \infty$) critical force statistics, where finite-size effects become negligible.

with $1 < \delta < 2$ (see figures 4 and 7), and consistent with the critical force distribution tail of the form $\ln P(f_c^s, L, M = k^*L) \sim -f_c^{s\delta}$ with $\delta = 1.2 \pm 0.1$ (see figure 6). When $k \simeq k^*$ the finite-size effects are small, but the convergence to the thermodynamic value displays the same scaling, $f_c - \langle f_c^s \rangle \propto L^{-(2-\zeta)}$.

doi:10.1088/1742-5468/2013/12/P12004


J. Stat. Mech. (2013) P12004

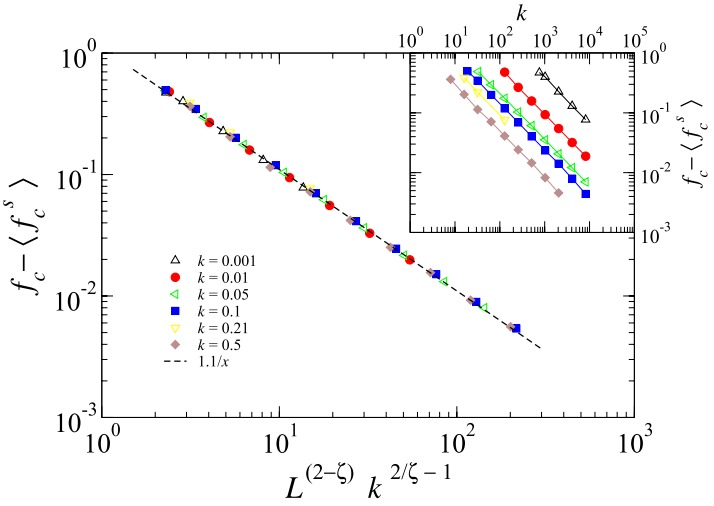


**Figure 4.** Negative finite-size bias of the critical force, $f_c - \langle f_c^s \rangle$, for small $k$ values. Inset: raw data. Main: scaled data. In this regime the shift is controlled exclusively by $M$ and by the RM depinning roughness exponent $\zeta$.

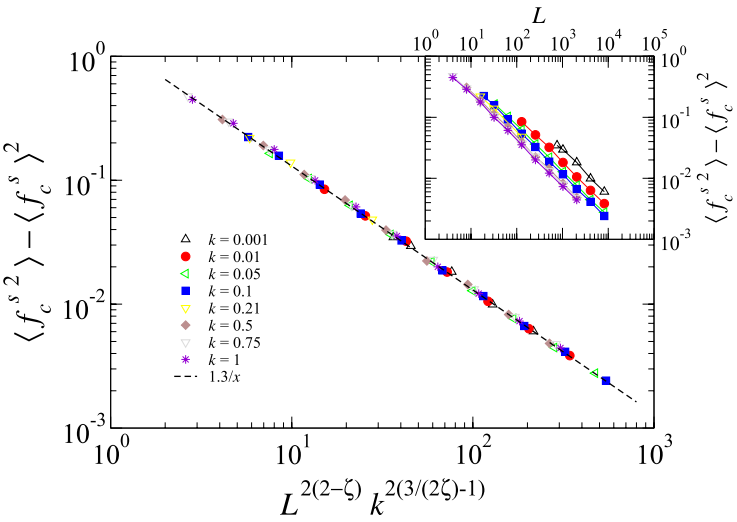


**Figure 5.** Finite-size fluctuations of the sample critical force, $\langle f_c^{s2} \rangle - \langle f_c^s \rangle^2$, for small $k$ values. Inset: raw data. Main: scaled data. In this regime the fluctuations are well described by $\langle f_c^{s2} \rangle - \langle f_c^s \rangle^2 \sim L^{-2(2-\zeta)} k^{2(1-3/2\zeta)}$. Note that in order to have a non-zero $\lim_{k\to 0}[\langle f_c^{s2} \rangle - \langle f_c^s \rangle^2]$, we need $\zeta \to 3/2$ in agreement with what corresponds to the (one-dimensional) RP class $[\langle f_c^{s2} \rangle - \langle f_c^s \rangle^2] \sim L^{-1}$ and roughness exponent $\zeta^{\mathrm{RP}} = 3/2$.

(3) The sample to sample fluctuations of the critical force are well described by

$$(\langle f_c^{s2} \rangle - \langle f_c^s \rangle^2) L^{2(2-\zeta)} \sim \begin{cases} k^{2(1-\zeta^{\mathrm{RP}}/\zeta)} & \text{if } k \ll k^* \\ (\log k)^{-2(1-1/\delta)} & \text{if } k \gg k^* \end{cases} \tag{5}$$

so they decrease with increasing $L$ or $k$ (see figures 5 and 8).

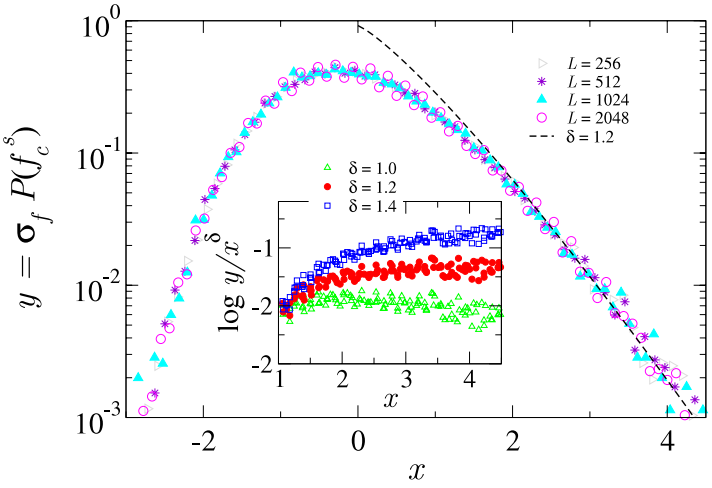


**Figure 6.** Scaled distribution function for the critical force, $y = \sigma_f P[f_c^s(k=2)]$, against $x = (f_c^s - \langle f_c^s \rangle)/\sigma_f$, with $\sigma_f = \sqrt{(\langle f_c^{s2} \rangle - \langle f_c^s \rangle^2)}$. Different system sizes are shown, $L \times M$ with $M = kL^\zeta$ for $k = 2$. The large $f_c^s$ tail can be fitted to a stretched exponential, $P(f_c^s) \sim \exp[-f_c^{s\delta}]$, characterized by $\delta = 1.2 \pm 0.1$, as can be observed in the inset.

(4) The width of the critical configuration behaves as

$$wL^{-\zeta} \sim \begin{cases} k^{-(\zeta^{\mathrm{RP}}/\zeta - 1)} & \text{if } k \ll k^* \\ (\log k)^{\zeta/2\delta} & \text{if } k \gg k^*. \end{cases} \tag{6}$$

The roughness thus always increases with increasing $L$ but has a non-monotonous behaviour with $k$, decreasing for small $k$ and increasing for large $k$. Its minimum is reached for a value $k \lesssim k^*$ (see figure 9).

### 3.2. The thermodynamic limit of the critical force

The existence of a *unique* critical force $f_c$ and velocity–force characteristics $v(f)$ (see section 3.4) for all finite values of $k$ shows that the transport properties of the QEW model have an unambiguous thermodynamic limit. In other words, the infinite family of systems described by (the same) equation (1) but with (different) geometries parametrized by the self-affine aspect-ratio parameter $k$, is attracted to a unique RM behaviour in the large-size limit (see figure 2). Note also that, even if $f_c$ and $v(f)$ are not universal, they are intrinsic; i.e., they depend only on the parameters appearing in the microscopic equation of motion.

*3.2.1. Finite-size effects for small k.* When $k$ is much smaller than $k^* \sim \mathcal{O}(1)$ (i.e. $M \ll L^\zeta$), the system can wrap around $M$ several times and, thus, sense the transverse periodicity of the disorder. Indeed, at a characteristic length $L_M \sim M^{1/\zeta} \ll L$ the geometry of the interface crosses over from the RM to the RP class, parametrized by the periodicity $M$. This crossover is well manifested in the structure factor $\langle |u_c(q)|^2 \rangle$ of the critical configuration, which displays [20], at $q \sim L_M^{-1}$, a crossover from the RM



J. Stat. Mech. (2013) P12004

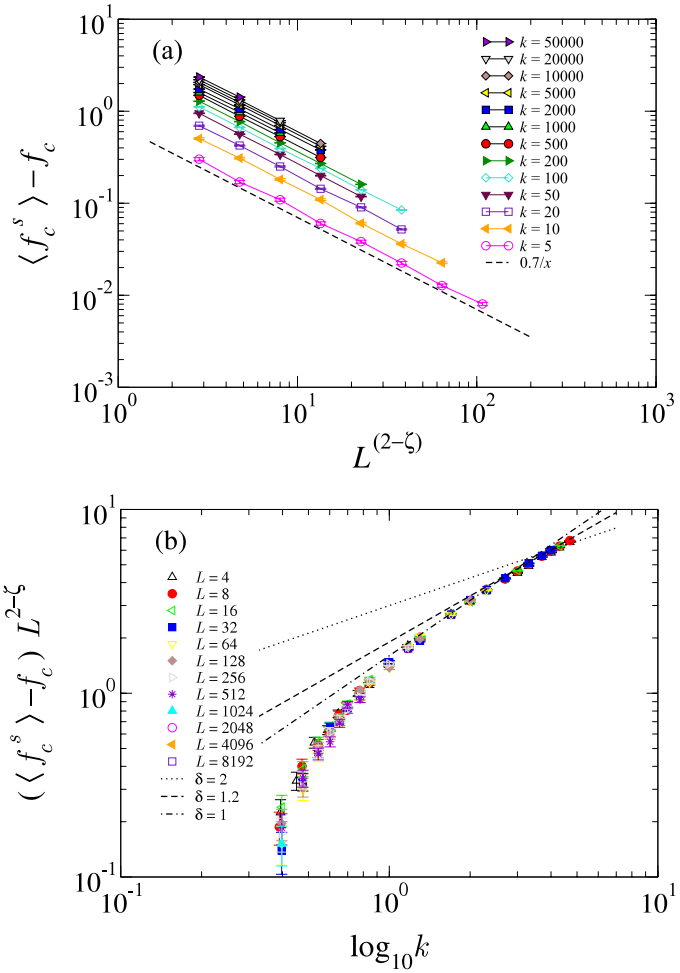


**Figure 7.** Positive finite-size shift of the critical force, $f_c - \langle f_c^s \rangle$, for large $k$. (a) The shift decays as $L^{-(2-\zeta)}$, with a $k$-dependent prefactor. (b) As expected from extreme value statistics, at the largest $k$ the shift increases with $k$ logarithmically, $f_c - \langle f_c^s \rangle \sim (\log k)^{1/\delta}$, with $\delta = 1.2$ in agreement with the tail exponent obtained in figure 6. We compare with $\delta = 2$ expected for the maximum of iid Gaussian random variables and $\delta = 1$ for the maximum of iid exponential variables.

roughness exponent $\zeta = 1.250$ (i.e., $\langle |u_c(q)|^2 \rangle \sim 1/q^{1+2\zeta}$) to the RP exponent[4] $\zeta^{\mathrm{RP}} = 3/2$ (i.e., $\langle |u_c(q)|^2 \rangle \sim 1/q^{1+2\zeta^{\mathrm{RP}}}$) when increasing the observation length-scale $q^{-1}$.

When $L$ grows with fixed $k$, $L_M$ grows as $L_M \sim k^{1/\zeta} L$. Since the average critical force $\langle f_c^s \rangle$ and velocity $\langle v^s \rangle$ for a finite system are determined by the typical behaviour at small length-scales ($l < L_M$) or short wavelength modes, the critical force must approach the RM thermodynamic value $f_c$ as $L_M$ grows, even when the large scale geometry ($l > L_M$) is still described by $\zeta^{\mathrm{RP}}$ instead of $\zeta$. Since, for our model of equation (1), the RP critical force $f_c^{\mathrm{RP}} \simeq \lim_{L\to\infty} \langle f_c^s(L, M) \rangle$ with $M \sim 1$ is always smaller that the RM critical force $f_c$, for small $k$ the thermodynamic limit is approached from *below*, as can be observed

[4] Note that $\zeta^{\mathrm{RP}} \equiv \zeta_{\mathrm{L}} = (4 - d)/2$ in $d = 1$, where $\zeta_{\mathrm{L}}$ is the Larkin exponent. This reflects the fact that the RP fixed point with $\zeta = 0$ is unstable due to a self-generated random force [35].



J. Stat. Mech. (2013) P12004

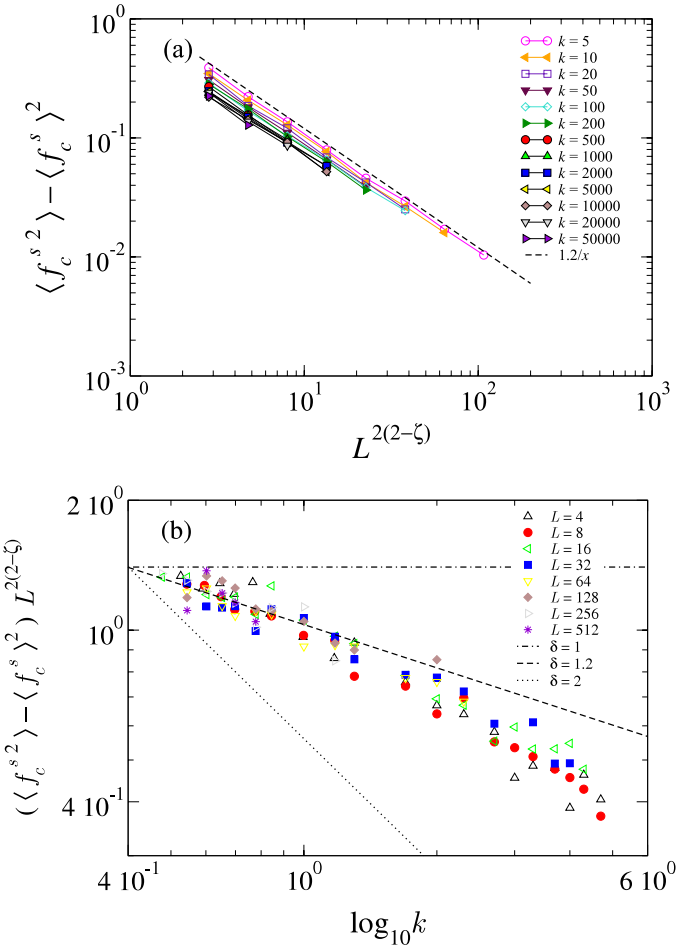


**Figure 8.** Finite-size fluctuations of the critical force $\langle f_c^{s2}\rangle - \langle f_c^{s}\rangle^2$, for large $k$. (a) $\langle f_c^{s2}\rangle - \langle f_c^{s}\rangle^2 \sim L^{-2(2-\zeta)}$, same as in the low $k$ regime (figure 5). (b) Dependence with $k$. We find $\langle f_c^{s2}\rangle - \langle f_c^{s}\rangle^2 \sim (\log k)^{-2(1-1/\delta)}$, consistent with the finite-size shift expected from extreme statistics. Note the consistency with $\delta = 1.2$ from figure 7.

in figures 2 and 3. Furthermore, we can see in figure 4 a negative finite-size bias of the critical force $f_c - \langle f_c^{s}\rangle$ for small values of $k$ that smoothly follows equation (4).

Let us introduce a heuristic argument to understand the scaling. In principle, one can think of the string as being composed of $L/L_M = k^{-1/\zeta} \gg 1$ 'RM blocks', of longitudinal size $L_M$ and transverse size $M$. Note that each of these blocks has precisely the 'proper' aspect ratio $L_M^{\zeta}/M = 1$. If we consider that each of these blocks participates in the total critical force with independent contributions, such that they average to $\overline{f_M}$ with a dispersion $\sigma_M$, where $\overline{\cdots}$ stands for an average over the independent RM blocks, then we can write:

$$\langle f_c^{s}(L,M)\rangle \approx \overline{f_M} \tag{7}$$

$$\langle f_c^{s2}(L,M)\rangle - \langle f_c^{s}(L,M)\rangle^2 \sim \frac{\sigma_M^2}{L/L_M}. \tag{8}$$

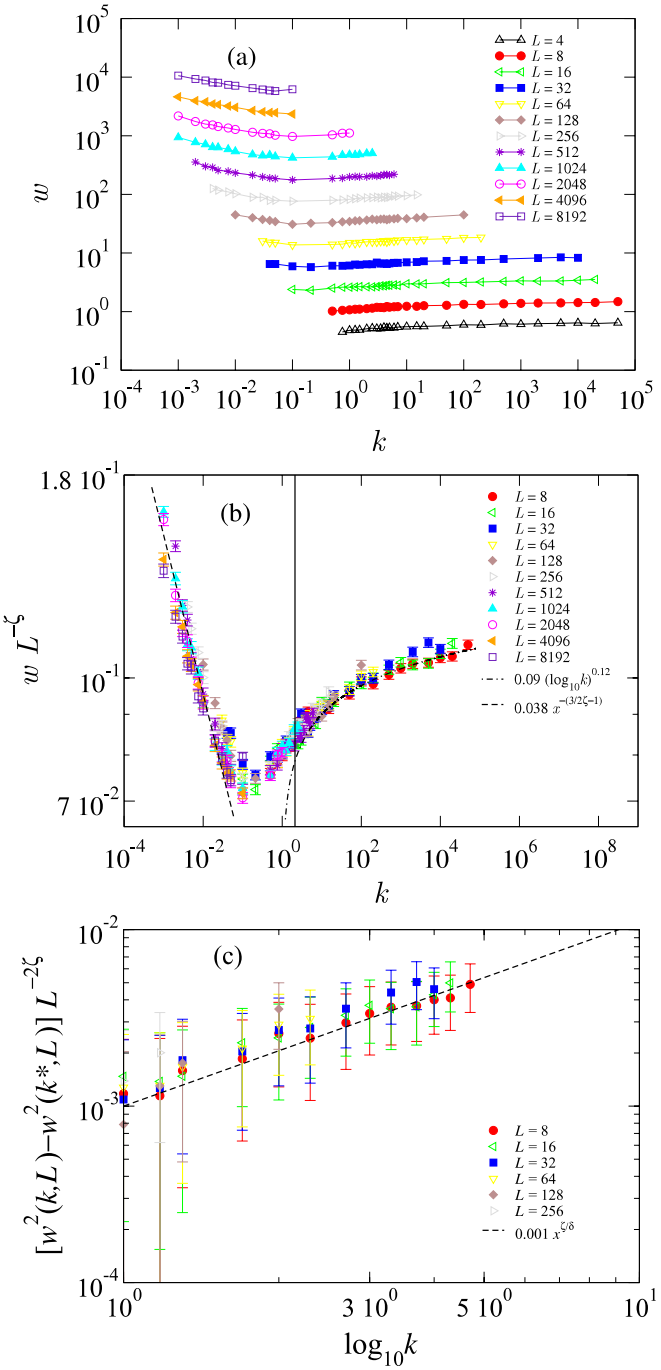


**Figure 9.** Anisotropic finite-size analysis of the width $w$ of the critical configurations. (a) Raw data. (b) Scaled data, according to $w \sim L^{\zeta}$, versus $k$. In the low $k$ regime, $w \sim L^{\zeta} k^{-(\zeta^{\mathrm{RP}}/\zeta - 1)}$ (dashed line). Note that for a non-zero $\lim_{k\to 0} w$ we need $\zeta \to \zeta^{\mathrm{RP}} = 3/2$, corresponding to the (one-dimensional) RP class (compare with the critical force fluctuations in the same regime shown in figure 4). The width for large $k$ is roughly described by some power-law of $\log k$ (dot-dashed line). The solid line indicates $k^* = 2.1$. (c) Scaled data, according to $[w^2(k,L) - w^2(k^*,L)] \sim L^{2\zeta} (\log k)^{\zeta/\delta}$ and using the values $\zeta = 1.250$ and $\delta = 1.2$, showing the agreement between the data and the scaling prediction.

J. Stat. Mech. (2013) P12004

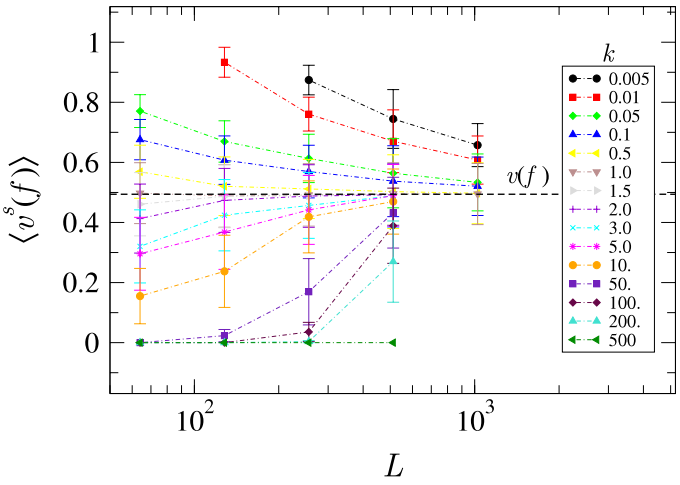


**Figure 10.** Finite-size effects in the mean velocity for different values of the self-affine aspect ratio $k$, and the same driving force $f = 1.95 > f_c$. We observe that velocity curves for finite $k$ values are attracted to the same limit $v(f) \approx 0.5$, except for $k = 500$, where rare blocking configurations still dominate and $f_c^s > f$ for the range of $L$ values analysed. The black dashed line indicates the estimation of the stationary velocity in the thermodynamic limit $\lim_{L\to\infty}\langle v^s(f)\rangle|_k \to v(f)$.

The above assumptions are consistent with the fact that $f_c^s$ has almost a Gaussian statistics [19] if $M \ll L^\zeta$, by virtue of the central limit theorem for the sum of many pinning forces with finite variance, which are uncorrelated at distances smaller than $L_M$. If $\overline{f_M}$ represents minus the average pinning force on a given block of size $L_M \times M$, then we can write $\overline{f_M} \sim f_c^s(L_M, M)$. Since the interface in each block is, by definition, in the RM regime, we can write $\sigma_M \sim L_M^{\zeta-2}$ for its sample to sample fluctuations. We thus get:

$$\langle f_c^s(L,M)\rangle \approx \langle f_c^s(L_M,M)\rangle \tag{9}$$

$$\langle f_c^{s2}(L,M)\rangle - \langle f_c^s(L,M)\rangle^2 \sim k^{2(1-3/2\zeta)} L^{-2(2-\zeta)}. \tag{10}$$

First, let us note that the predicted finite-size scaling dependence on $L$ and $k$ for $\langle f_c^{s2}(L,M)\rangle - \langle f_c^s(L,M)\rangle^2$ is indeed what we observe in figure 5. Second, let us note that $\langle f_c^s\rangle$ depends only on $M$ (as $L_M = M^{1/\zeta}$), consistent with the behaviour shown in figure 4. If this bias scales with the longitudinal size in the same way as the sample to sample fluctuations, one can predict $[f_c - \langle f_c^s(L,M)\rangle] \approx [f_c - \langle f_c^s(L_M,M)\rangle] \sim L_M^{\zeta-2} \sim M^{2/\zeta-1} \sim L^{-(2-\zeta)} k^{(1-2/\zeta)}$, as shown in figure 4.

It is interesting to note that in order to have $\lim_{k\to 0}\left[\langle f_c^{s2}(L,M)\rangle - \langle f_c^s(L,M)\rangle^2\right] \sim k^{2(1-3/2\zeta)} L^{-2(2-\zeta)}$ finite in the $L \to \infty$ thermodynamic limit, which corresponds to the RP class with a fixed periodicity $M$, we require that $\zeta \to \zeta^{\mathrm{RP}} = 3/2$. Therefore, $\langle f_c^{s2}(L,M)\rangle - \langle f_c^s(L,M)\rangle^2 \sim L^{-1}$, again consistent with the prediction for the critical force fluctuations in the RP class.

*3.2.2. Finite-size effects for large $k$.* When $k$ is large, periodicity effects disappear, since the critical configuration cannot wind around the cylinder of perimeter $M$. In turn, we start to observe *extreme value statistics* effects. As described in [19], in the $k \to \infty$ limit



J. Stat. Mech. (2013) P12004

the critical force distribution tends to a Gumbel function; i.e., the critical force of each sample can be thought of as the maximum of independent identically distributed (iid) variables with a (stretched) exponential-tailed distribution. This explains why $\langle f_c^s(L,M)\rangle$ approaches $f_c$ from above in figure 2. Indeed, considering $\langle f_c^s\rangle$ as the maximum among the critical forces of many independent configurations we can expect a growth with increasing $M$ at $L$ fixed, which is observed in figure 3. Since metastable (or quasi-critical) configurations just below (or above) the depinning transition are essentially decorrelated in a distance of the same order as its width $w \simeq L^\zeta$ (as argued in [28]), the number of such independent random variables is precisely $k = M/L^\zeta$.

Let us analyse the case when $k$ is finite and close to $k^*$. On one hand, in this case finite-size effects are less pronounced, as shown in figure 2. We can expect that, in the same sense that $f_c^s$ is attracted to $f_c$, the distribution function should also be attracted to a thermodynamic limit which would be close to the one with $k = k^*$. Note that the critical force $f_c^s$ of a system of size $L \times k^* L^\zeta$ is distributed according to a function which is intermediate between the Gaussian and the Gumbel [19]. Although the shape of this function is not known analytically, we know that it must decay faster than a power-law, since the maximum among $k = M/L^\zeta$ of such systems is attracted to the Gumbel class in the $k \to \infty$ limit. In fact, this effect was recently observed for the cumulative distribution of thresholds in the discrete version of the model [28]. To support this idea, let us consider the tail of $P(f_c^s)$ described in particular as a stretched exponential decay, $\ln P(f_c^s) \sim -f_c^{s\delta}$, with $1 \leq \delta \leq 2$ (the bounds corresponding to the Gaussian case, $\delta = 2$, and to the Gumbel case, $\delta = 1$). We show in figure 6 the distribution function for the sample critical force $f_c^s$ corresponding to $k = 2$, where the system size effects are almost negligible. It is shown in this case that the tail exponent characterizing the stretched exponential behaviour is $\delta = 1.2 \pm 0.1$. The same exponent $\delta$ is observed for different values of $k$ and we expect it to be universal, as are the critical exponents $\zeta, \nu, \beta$, etc. It would be interesting to check that $\delta$ is not affected by the presence of a different disorder distribution or geometry[5].

Therefore, based on the observed stretched exponential behaviour and from standard extreme value statistics arguments [36] we get that the average of $f_c^s = \max\{f_1^{(0)}, f_1^{(1)}, \ldots, f_1^{(k)}\}$ should grow as $\langle f_c^s\rangle - f_c \sim L^{-(2-\zeta)}(\log k)^{1/\delta}$. Here we have used again that the finite-size bias for a $L \times L^\zeta$ (or $k \sim 1$) system behaves as the sample to sample fluctuations $\langle f_1\rangle - f_c \sim L^{-(2-\zeta)}$ in the $L \to \infty$ limit. This prediction is consistent with what is found in the simulations, as shown in figure 7. The large $k$ behaviour is consistent with the obtained value of the tail exponent $\delta = 1.2$. Within this picture, standard extreme value arguments also predict $\langle f_c^2\rangle - \langle f_c^s\rangle^2 \sim L^{-2(2-\zeta)}(\log k)^{-2(1-1/\delta)}$. This is also consistent with figure 8, where we compare the prediction using the same value of $\delta$ as obtained in figure 6. As can be observed in figure 8(b), in the large $L$ limit the data is consistent with the value of $\delta = 1.2 \pm 0.1$, ruling out the bounds $\delta = 2$ for the maximum of iid Gaussian variables, and $\delta = 1$ for the maximum of iid exponential variables.

It is interesting to note that since $\delta > 1$ the sample to sample fluctuations of the critical force *decrease* for increasing $k$, unlike the mean value of the critical force, which *increases* with $k$. Therefore, the growing sample critical force reaches a sharply defined value in the large $k$ limit. This might be important for experiments.

[5] Note that in statics the value of $\delta$ characterizing the tails of the free energy is well known. In particular, for $d = 1$, $\delta = 3/2$ for all boundary conditions, and this value is one of the fingerprints of the Tracy–Widom family.



J. Stat. Mech. (2013) P12004

### 3.3. Finite-size effects in the roughness of the critical configuration

The typical interface global width or roughness also manifests size effects at depinning, which are consistent with the finite-size scaling for the critical force.

Let us first describe the low-$k$ behaviour of the width $w$ shown in figure 9. From the study of the RM to RP crossover at $L_M \sim M^{1/\zeta} \ll L$ we know that [20] $w(L) \sim L_M^{\zeta}(L/L_M)^{\zeta^{\mathrm{RP}}}$. We thus get

$$w(L) \sim k^{-(\zeta^{\mathrm{RP}}/\zeta-1)} L^{\zeta} \tag{11}$$

consistent with the asymptotic behaviour shown in figure 9(b) for small values of $k$, where $\zeta^{\mathrm{RP}} = 3/2$ for our one-dimensional case.

Turning now to the behaviour of the roughness critical configurations at large values of $k$, we can see that, interestingly, it displays an approximate logarithmic growth with $k$, as shown in figure 9(b). This was already observed in [24]. Here we link such behaviour with the critical force statistics and predict its scaling form. We start by noting that in order to have a logarithmic growth of $f_{\mathrm{c}}^{\mathrm{s}}$ with $k$ in this regime, either the individual pinning forces on the monomers of the critical configuration get more correlated in order to increase $f_{\mathrm{c}}^{\mathrm{s}}$, or they remain uncorrelated but acquire an enhancement of their dispersion with increasing $k$. Since we do not observe increased correlations between the individual pinning forces acting on the monomers of $u_{\mathrm{c}}$ for large $k$, the last scenario is the most plausible. A logarithmic enhancement in the prefactor $w^2/L^{\zeta}$ can thus be heuristically understood as follows. From the Larkin formulation we can define effective Larkin length $L_{\mathrm{c}} \sim (f_{\mathrm{c}}/cr_f)^{-1/2}$ and roughness $w \approx r_f(L/L_{\mathrm{c}})^{\zeta}$. Extending this idea to sample fluctuations, we consider that $\langle L_{\mathrm{c}}^s(k,L)\rangle \sim (\langle f_{\mathrm{c}}^{\mathrm{s}}\rangle/cr_f)^{-1/2}$ and $w \approx r_f(L/\langle L_{\mathrm{c}}^s\rangle)^{\zeta}$. Therefore, using that $\langle f_{\mathrm{c}}^{\mathrm{s}}\rangle - f_{\mathrm{c}} \sim (\log k)^{1/\delta}$ we easily get $w(k,L)/L^{\zeta} \sim (\log k)^{\zeta/2\delta}$ in the very large $k$ limit, where $\langle f_{\mathrm{c}}^{\mathrm{s}}\rangle \gg f_{\mathrm{c}}$. Since our data does not reach such a limit, we cannot neglect the $f_{\mathrm{c}}$ contribution. A corrected version reads $(w(k,L)/L^{\zeta})^2 - (w(k^*,L)/L^{\zeta})^2 \sim (\log k)^{\zeta/\delta}$, where we have used the $k$-independent thermodynamic limit $\lim_{L\to\infty} w(k,L)/L^{\zeta} \approx w(k^*,L)/L^{\zeta} \sim r_f L_{\mathrm{c}}^{-\zeta}$. Figure 9(c) presents a scaled version of the data to test this idea, where we have used that $\zeta = 1.250$, $\delta = 1.2$ (see fit in figure 7) and $k^* \approx 2$ (see figure 3), and shows a very good agreement with the scaling prediction.

In summary, the increasingly rare critical configurations for large $k$ can be thus seen as being pinned by an effectively stronger uncorrelated microscopic disorder keeping the same elasticity and microscopic disorder correlator range. In other words, extreme statistics shorten the effective Larkin length on those critical configurations.

### 3.4. Finite-size effects in the velocity–force characteristics

When $f > f_{\mathrm{c}}^{\mathrm{s}}$, the elastic interface moves steadily with velocity $v^s(f)$ and the geometry displays a crossover in the roughness from the exponent $\zeta$ to the exponent $\zeta^{\mathrm{th}} = (2-d)/2$ at the characteristic scale $\xi \sim v^{-\nu/\beta}$. Given the presence of this extra length-scale depending on the force excess, it is not obvious whether the same thermodynamic limit prescription for the RM critical force (i.e., to fix the aspect-ratio parameter $k = ML^{-\zeta}$) will work for the velocity, yielding a unique $k$-independent velocity limit $v(f)$.

In figure 10 we show that the prescription for $f_{\mathrm{c}}$ works well for $v(f)$. We observe that a wide range of values of $k$ tends to converge to a $k$-independent, force dependent steady-state velocity, $\lim_{L\to\infty}\langle v^s(f;k,L)\rangle|_k \to v(f)$. At finite $L$, we observe that $\langle v^s(f)\rangle > v(f)$



J. Stat. Mech. (2013) P12004

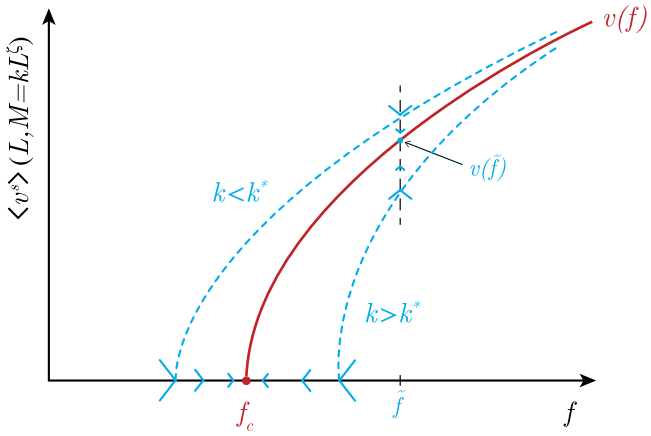


**Figure 11.** Schematic $k$-dependence of the velocity–force characteristics. For $k > k^*$ the critical force bias is positive, $f_c^s < f_c$, and therefore the velocity at a given force $f > f_c$ approaches the thermodynamic limit from below, $\langle v^s(f)\rangle < v(f)$. The opposite is observed when $k < k^*$: the critical force bias is negative and hence the velocity is $\langle v^s(f)\rangle > v(f)$.

for small $k$, and $\langle v^s(f)\rangle < v(f)$ for large $k$. This is consistent with the behaviour of the finite-size average critical force (see schema in figure 11): $f_c^s$ is biased to greater values of $f$ as $k$ increases above $k^*$, so, if we assume a monotonous and continuous behaviour of the velocity–force curve, for a given $f$ the velocity average $\langle v^s(f)\rangle$ should be smaller as $k > k^*$ increases. Indeed, for very large $k$, we can be in the situation where $f < f_c^s$ and thus $\langle v^s\rangle = 0$, as is seen in figure 10 for $k = 500$. On the other hand, for small values of $k < k^*$, $f_c^s$ decreases with $k$, and at a fixed force $f$ the average velocity will be larger as $k$ decreases. This is why curves for $k < k_v^* \simeq 1 \sim k^*$ converge from *above* in figure 10 to the thermodynamic limit.

In figure 12 we observe the behaviour of $\langle v^s(f)\rangle$ as a function of $k$ for different system sizes. For the working force $f = 1.95 > f_c$, a crossing of all curves at $k_v^* \simeq 1$ can be observed, but also, how curves are apparently attracted to a unique constant value, both above and below $k_v^*$, as $L$ increases. We find that $k_v^* \sim \mathcal{O}(1)$, without appreciably varying with $f$. This shows that the same critical force prescription is adequate to obtain the thermodynamic limit of the velocity–force curve, and that finite-size effects at any finite $k$ vanish as $L \to \infty$.

## 4. Discussion

### 4.1. Comparison with the velocity-driven ensemble

In this paper we have defined the critical force of a one-dimensional QEW line in a given finite disorder sample of dimensions $L \times M$ with periodic boundary conditions in all directions, driven by a uniform, constant force $f$. In some situations, however, the interface is velocity-driven in a infinitely wide medium, and the driving force $f$ is replaced by a term $m^2[vt - u(x,t)]$, with $v$ the imposed mean velocity. We will argue that the results of equations (4), and (5) are also relevant for this case, and that a close connection exists simply by relating the curvature parameter $m$ and the transverse periodic dimension $M$.



J. Stat. Mech. (2013) P12004

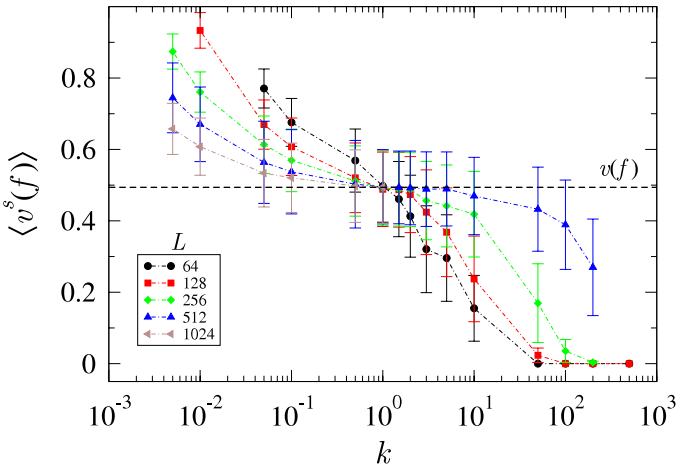


**Figure 12.** Same data as in figure 10 but showing the transverse finite-size dependence, for each $L$, of the averaged stationary velocity. Note the crossing at $k_v^*$, where finite-size effects become negligible, bridging the Gaussian ($k \to 0$) with the Gumbel ($k \to \infty$) statistics.

Since the parabolic drive sets a characteristic length-scale $L_m \sim 1/m$ in the longitudinal direction, we can compare it directly with the length $L_M \sim M^{1/\zeta}$ set by the periodic boundary conditions in the constant force simulations. We can hence relate $M^{1/\zeta}$ and $1/m$, so the limit of small $m$ corresponds to the large $M$ limit, and vice versa.

The critical force is defined in the quasistatic limit of the velocity-driven interface as $\langle f_c^s(L,m)\rangle \equiv \lim_{v\to 0+} m^2\langle [vt - u(x,t)]\rangle$ for stationary values of $u(x,t)$. It can be compared with the critical force $\langle f_c^s(L,M)\rangle$ discussed in the previous subsections. Functional Renormalization group (FRG) calculations predict when $L \to \infty$ that $\langle f_c^s(m)\rangle = f_c + c_1 m^{2-\zeta}$ in the small $m$ limit, with $c_1$ a negative constant and $f_c$ the thermodynamic critical force. If we assume $L$ very large and define $k_m = (Lm)^{-\zeta}$, such a prediction reads $\langle f_c^s(m)\rangle = f_c + c_1 k_m^{1-2/\zeta} L^{\zeta-2}$. As shown in equation (4), this is exactly the same scaling we find for $\langle f_c^s(L, M = kL^\zeta)\rangle$ for small $k$, with $f_c > \langle f_c^s(m)\rangle$ assured by the FRG prediction $c_1 < 0$. This supports our identification of $k$ with $k_m$, and we can expect equations (4) and (5) to hold in the velocity-driven ensemble by replacing $k \mapsto k_m$.

To further emphasize the connection we note that the numerical extrapolation of $\langle f_c^s(m)\rangle$ in the velocity-driven ensemble yields a value [37] $f_c \sim 1.9$, indistinguishable from ours, $f_c \approx 1.916 \pm 0.001$, for the same microscopic disorder. On the other hand, the prediction $\langle f_c^s(m)\rangle = f_c + c_1 k_m^{1-2/\zeta} L^{\zeta-2}$ shows that for small $k_m$ (i.e. large $m$ compared to $L^{-1}$), the critical force is smaller than $f_c$, as we see in figure 4 for small $k$. Moreover, as shown in figure 2 of [37], when $k_m$ is large (i.e., $m$ small compared to $L^{-1}$), $f_c^s(m)$ can become larger than the extrapolated $f_c$. This is due to extreme value statistic effects similar to the ones discussed in the previous sections: as the curvature of the parabola vanishes for a fixed $L$, the interface can get blocked in rarer configurations with systematically higher critical forces.

In summary, the transport properties have a unique limit and similar finite-size effects in the two ensembles. Only the roughness of the critical configurations for small $k$ or $k_m$ are different, since for the velocity-driven case, the roughness beyond the length-scale $L_m \sim 1/m$ crosses over from $\zeta \approx 1.25$, to $\zeta^{\mathrm{m}} = 0$ (instead of $\zeta^{\mathrm{RP}} = 3/2$), so $w \sim m^{-\zeta}$.



J. Stat. Mech. (2013) P12004

On the other hand, for small $m$, such that $mL \ll 1$, we expect to observe a behaviour analogous to equation (6) for large $k$. This has not been analysed yet in the velocity-driven ensemble.

Finally, it is worth mentioning that an original alternative approach was analytically implemented in [23], by defining a critical force for a fixed centre of mass position. This choice avoids rare configurations as the interface cannot explore the disorder in the transverse directions beyond the length-scale set by its own width $w \sim L^{\zeta}$. It is thus equivalent to working with a system size satisfying $k \sim 1$ (or $k_m \sim 1$), and must thus have the same unique thermodynamic limit. The advantage of this method is that it is parameter free, and size effects are controlled only by $L$. In addition, it does not present crossovers, and the critical configuration geometry always belongs to the (non-extreme) RM class. However, so far this method has been implemented only analytically.

### 4.2. Implications for the non-steady universal relaxation of the velocity

It is interesting to relate the finite-size bias of the critical force, equation (4), with the universal non-steady relaxation at the thermodynamic depinning threshold [38]. In [34] it was noted that the short-time relaxation of an initially flat interface *at the RM thermodynamic critical force* $f_c$ can be effectively described as an interface of 'size' $\ell(t)$ which is quasistatically driven by the finite-size bias of the critical force. That is, we assume that $v(t)$ instantaneously satisfies the steady-state relation $v(t) \sim [f_c - f_c(\ell(t))]^{\beta}$, where the effective 'size' grows with time as the growing correlation length $\ell(t) \sim t^{1/z}$, with $z$ the dynamical exponent. By assuming $f_c - f_c(\ell(t)) \sim \ell(t)^{\zeta-2}$, we get the critical relaxation $v(t) \sim t^{-\beta/\nu z}$.

The finite-size scaling of equation (4) allows us now to better justify the above assumptions. The initially flat relaxing string of size $L$, in the small (non-steady) velocity limit such that the adiabatic approximation holds, effectively becomes a (pseudo) critical configuration confined in a system of effective size $L \times w(t)$. This situation is equivalent to the one described in section 4.1 with $m(t) \sim w(t)^{-1/\zeta}$, in the quasistatic drive limit. This defines an effective aspect-ratio parameter $k(t) \sim w(t)/L^{\zeta} \ll k^*$, and allows us to write,

$$v(t) \sim [f_c - f_c(L, k(t))]^{\beta} \sim k(t)^{\beta(1-2/\zeta)} \sim t^{-\beta/\nu z}, \tag{12}$$

where in the second term we have used the $k \ll k^*$ scaling for the bias of the critical force, equation (4), and in the third term the STS relation $\nu = 1/(2-\zeta)$. When $k(t) \sim k^*$ the bias vanishes, corresponding to the vanishing of the velocity in a finite system when [38] $\ell(t) \sim L$. The string is then blocked by a *typical* RM critical configuration. In order to explore rare critical configurations we need to drive the system above the thermodynamic critical force $f > f_c$. Then, from equation (4), and the same adiabatic approximation for $v(t)$, we can expect a crossover to a new regime in the non-steady relaxation, from a power-law to a slower logarithmic decay.

## 5. Conclusions

We have shown that there exists a unique, unambiguous thermodynamic limit for the transport properties of driven elastic interfaces in random media, irrespective of the precise relation between the longitudinal and transverse dimensions of the system, only



J. Stat. Mech. (2013) P12004

provided they maintain a definite scaling relation in the large-size limit. Namely, any finite value of the self-affine aspect-ratio parameter $k = M/L^{\zeta}$, with $\zeta \simeq 1.250$ the depinning exponent, leads to exactly the same transport properties in the large-size limit. We have also characterized in detail the finite-size effects in the critical force fluctuations for small and large values of $k$. Our results thus extend the ones of [19] in several useful ways. In particular, we show that the thermodynamic critical force is not only finite if $k$ is finite, but that it is independent of $k$; i.e., it is *unique*. We also report a finite-size bias or shift in the critical force, which was unnoticed before, as, in general, only reduced variables (of zero mean) were analysed. We give good evidence that the velocity–force characteristics is itself a *unique* curve in the thermodynamic limit, and interpret it as an attractor for the stationary and even non-stationary behaviour of any finite system with well defined geometry. Finally, we have also shown that our results are completely consistent with the ones obtained for velocity-driven interfaces, where $f \to m^2(vt - u(x,t))$, so the two ensembles have the same transport properties in the thermodynamic limit and are thus equivalent.

## Acknowledgments

ABK and AR acknowledge partial support by the France–Argentina MINCYT-ECOS A12E05. EEF acknowledges partial support by the France–Argentina Bernardo Houssay Program 2012. SB acknowledges partial support by the France–Argentina MINCYT-ECOS A12E03. Partial support from Project PIP11220090100051 (CONICET) and Project PICT2010/889 are also acknowledged.

## References

[1] Lemerle S, Ferré J, Chappert C, Mathet V, Giamarchi T and Le Doussal P, 1998 *Phys. Rev. Lett.* **80** 849
[2] Bauer M, Mougin A, Jamet J P, Repain V, Ferré J, Stamps R L, Bernas H and Chappert C, 2005 *Phys. Rev. Lett.* **94** 207211
[3] Yamanouchi M, Chiba D, Matsukura F, Dietl T and Ohno H, 2006 *Phys. Rev. Lett.* **96** 096601
[4] Metaxas P J, Jamet J P, Mougin A, Cormier M, Ferré J, Baltz V, Rodmacq B, Dieny B and Stamps R L, 2007 *Phys. Rev. Lett.* **99** 217208
[5] Lee J-C, Kim K-J, Ryu J, Moon K-W, Yun S-J, Gim G-H, Lee K-S, Shin K-H, Lee H-W and Choe S-B, 2011 *Phys. Rev. Lett.* **107** 067201
[6] Paruch P, Giamarchi T and Triscone J M, 2005 *Phys. Rev. Lett.* **94** 197601
[7] Paruch P and Triscone J M, 2006 *Appl. Phys. Lett.* **88** 162907
[8] Jo J Y, Yang S M, Kim T H, Lee H N, Yoon J-G, Park S, Jo Y, Jung M H and Noh T W, 2009 *Phys. Rev. Lett.* **102** 045701
[9] Paruch P, Kolton A B, Hong X, Ahn C H and Giamarchi T, 2012 *Phys. Rev.* B **85** 214115
[10] Guyonnet J, Agoritsas E, Bustingorry S, Giamarchi T and Paruch P, 2012 *Phys. Rev. Lett.* **109** 147601
[11] Moulinet S, Rosso A, Krauth W and Rolley E, 2004 *Phys. Rev.* E **69** 035103(R)
[12] Le Doussal P, Wiese K J, Moulinet S and Rolley E, 2009 *Europhys. Lett.* **87** 56001
[13] Bouchaud E, Bouchaud J P, Fisher D S, Ramanathan S and Rice J R, 2002 *J. Mech. Phys. Solids* **50** 1703
[14] Bonamy D, Santucci S and Ponson L, 2008 *Phys. Rev. Lett.* **101** 045501
[15] Parkin S S P, Hayashi M and Thomas L, 2008 *Science* **320** 190
[16] Ohno H, 2010 *Nature Mater.* **9** 952
[17] Kim K-J, Lee J-C, Ahn S-M, Lee K-S, Lee C-W, Cho Y J, Seo S, Shin K-H, Choe S-B and Lee H-W, 2009 *Nature* **458** 740
[18] Cule D and Hwa T, 1998 *Phys. Rev.* B **57** 8235
[19] Bolech C J and Rosso A, 2004 *Phys. Rev. Lett.* **93** 125701
[20] Bustingorry S, Kolton A B and Giamarchi T, 2010 *Phys. Rev.* B **82** 094202



J. Stat. Mech. (2013) P12004

[21] Barabási A-L and Stanley H E, 1995 *Fractal Concepts in Surface Growth* 1st edn (Cambridge: Cambridge University Press)
[22] Bustingorry S, Kolton A B and Giamarchi T, 2012 *Phys. Rev.* B **85** 214416
[23] Fedorenko A A, Le Doussal P and Wiese K J, 2006 *Phys. Rev.* E **74** 041110
[24] Bustingorry S and Kolton A B, 2009 *Papers Phys.* **2** 1
[25] Le Doussal P and Wiese K J, 2009 *Phys. Rev.* E **79** 051105
[26] Middleton A A and Fisher D S, 1993 *Phys. Rev.* B **47** 3530
[27] Narayan O and Fisher D S, 1992 *Phys. Rev.* B **46** 11520
[28] Budrikis Z and Zapperi S, 2013 *J. Stat. Mech.* P04029
[29] Kolton A B, Rosso A, Giamarchi T and Krauth W, 2006 *Phys. Rev. Lett.* **97** 057001
[30] Kolton A B, Rosso A, Giamarchi T and Krauth W, 2009 *Phys. Rev.* B **79** 184207
[31] Ferrero E E, Bustingorry S, Kolton A B and Rosso A, 2013 *C.R. Phys.* **14** 641
[32] Rosso A and Krauth W, 2002 *Phys. Rev.* E **65** 025101
[33] Rosso A and Krauth W, 2001 *Phys. Rev. Lett.* **87** 187002
[34] Ferrero E E, Bustingorry S and Kolton A B, 2013 *Phys. Rev.* E **87** 032122
[35] Le Doussal P, Wiese K J and Chauve P, 2002 *Phys. Rev.* B **66** 174201
[36] Galambos J, 1987 *The Asymptotic Theory of Extreme Order Statistics* (Malabar, FL: Krieger)
[37] Rosso A, Le Doussal P and Wiese K J, 2007 *Phys. Rev.* B **75** 220201(R)
[38] Kolton A B, Rosso A, Albano E V and Giamarchi T, 2006 *Phys. Rev.* B **74** 140201

J. Stat. Mech. (2013) P12004